

Likelihood Inference for Non-Linear, Multivariate Jump Diffusions With State-Dependent Intensity

Etienne A.D. Pienaar*

Department of Statistical Sciences, University of Cape Town, Rondebosch, Cape Town 7707, South Africa.

e-mail: etiennead@gmail.com

and

Melvin M. Varughese*

Department of Statistical Sciences, University of Cape Town, Rondebosch, Cape Town 7707, South Africa.

e-mail: melvin.varughese@uct.ac.za

Abstract: Jump diffusion processes provide a means of modelling both small and large deviations in continuously evolving processes. Unfortunately, the calculus of jump diffusion processes makes it difficult to analyse non-linear models. This paper develops a method for approximating the transition densities of time-inhomogeneous multivariate jump diffusions with state-dependent and/or stochastic intensity. By deriving a system of equations that govern the evolution of the moments of the process, we are able to approximate the transitional density through a density factorization that contrasts the dynamics of the jump diffusion with that of its jump free counterpart. Within this framework we develop a class of quadratic jump diffusions for which we can calculate accurate approximations to the likelihood function. Subsequently, we analyse a number of non-linear jump diffusion models for Google equity volatility, alternating between various drift, diffusion, and jump mechanism specifications. In doing so we find evidence of both cyclical drift and a state-dependent jump mechanism.

MSC 2010 subject classifications: Primary 60H10, 60J60, 60J75; secondary 60J65, 62E17.

Keywords and phrases: Jump Diffusion Process, Markov Chain Monte Carlo, Kolmogorov Equation, Inference, Jump Stochastic Differential Equation.

Contents

1	Introduction	1
2	Multivariate jump diffusions with state-dependent jump intensity . . .	5
3	Approximating the transitional density of a jump diffusion	10
	3.1 Deriving a partial difference differential equation for the moment generating function	10

*Etienne Pienaar and Melvin Varughese were both funded by the National Research Foundation of South Africa.

3.2 Moment equations and the generalised quadratic jump diffusions 13

3.3 A Scalar Example 20

3.4 Short time scale dynamics and the excess factorization 25

4 Benchmarking and comparison to existing methods 34

4.1 Brownian motion with drift: Short time approximations of the transitional density 34

4.2 State dependent models: Characteristic equations 42

5 Likelihood inference 46

5.1 Exact vs. approximate likelihoods 47

5.2 Likelihood inference for non-linear processes 51

5.3 Bivariate, coupled process with Normally distributed jumps. 55

6 Application to Google stock price volatility 57

7 Conclusion 62

Acknowledgements 62

Appendices 62

A Simplification of the PDDE for the moment generating function 62

B Derivation of series expressions for $C_i(\alpha, \beta)$ i.t.o. $M_i^*(\alpha, \beta)$ 64

C Moment and cumulant relations 66

D Moment Equations of a Bivariate CIR Jump Process With Time-Inhomogeneous Jump Variables 67

E Surrogate Densities 68

References 69

1. Introduction

Real world processes are often subject to numerous sources of random input, resulting in multifarious random behaviour that forms an integral part of the trajectory of the process. In modelling such phenomena, it is thus imperative that the model equations account for the various sources of randomness that govern the dynamics of the process. Although diffusion processes are used extensively in the modelling of continuous processes, it is usually assumed that Brownian motion suffices as driving mechanism for the stochastic evolution of the processes. Where it does not suffice, it is possible to generalise the model process in order to make it more realistic for the application at hand. One such generalisation is to include randomly occurring ‘jumps’ in the trajectory of the model process. This modification has primarily been motivated in financial contexts where diffusion models are used to describe the dynamics of price/asset processes which are subject to seemingly spontaneous yet frequent jumps in observed time series. For example, it is often assumed that log-returns on a given stock-price process are Normally distributed. This assumption can easily be accommodated in an stochastic differential equation by assuming that the dynamics of the stock-price process follows that of geometric Brownian motion:

$$dX_t = \mu X_t dt + \sigma X_t dB_t, \tag{1.1}$$

where X_t denotes the stock price at time t , from which it follows that $\log(X_t) - \log(X_s) \sim N((\mu - \sigma^2/2)(t - s), \sigma^2(t - s))$ for $t > s$. However, the normality of stock-price returns have long been contested, and empirical evidence suggests that returns often exhibit features which are not well replicated by the Normal distribution. Perhaps the most well documented of these is the apparent lack of heavy tails in the model process. This is demonstrated by calculating descriptive statistics such as the skew and kurtosis of the observed return series, which may subsequently be contrasted to the corresponding statistics under the Normal distribution. In the context of diffusion processes, this disparity is typically compensated for by formulating a stochastic volatility model wherein the diffusion coefficient of the returns process is itself treated as a stochastic process. That is, the revised process may for example assume the form:

$$\begin{aligned} d\log(X_t) &= \left(\mu - \frac{1}{2}\sigma_t^2\right)dt + \sigma_t dB_t^{(1)} \\ d\sigma_t^2 &= a(\sigma_t^2, t)dt + b(\sigma_t^2, t)dB_t^{(2)}, \end{aligned} \tag{1.2}$$

where $a(\sigma_t^2, t)$ and $b(\sigma_t^2, t)$ denote the drift and diffusion of the variance process respectively, and $B_t^{(1)}$ and $B_t^{(2)}$ are correlated Brownian motions. Among numerous other attractive properties, stochastic volatility models make it possible to more accurately capture the tail behaviour of the stock-price returns by explicitly allowing the variance of the log-returns to vary over time, resulting in a significantly improved approximation of the observed process. However, care needs to be taken when interpreting the stochastic volatility mechanism. Indeed, when $B_t^{(1)}$ and $B_t^{(2)}$ are uncorrelated the marginal distribution of the log-returns process conditional on a known initial value for the variance process (i.e., $X_t|X_s, \sigma_s^2$ for $t > s$) is still Normal, and even when strong correlation is present, in which case the marginal distribution of log-returns may be skew with slightly fatter tails than predicted under the Normal distribution, the resulting transitional density may not be sufficiently leptokurtic to account for extreme return events over short transition horizons. To illustrate the point, consider a rolling estimate of kurtosis for daily log-returns of the Standard and Poor's 500 index (S&P 500). Let X_{t_i} denote the value of the S&P 500 index at time t_i , then define a backward-looking rolling estimate of kurtosis with bandwidth h by:

$$K(t_i, h) = \frac{1}{h \times \hat{s}^2(t_i, h)} \sum_{k=i-h+1}^i \left(X_{t_k} - \hat{m}(t_i, h) \right)^4 \tag{1.3}$$

for all $i \geq h$, where $\hat{s}(t_i, h) = \frac{1}{h} \sum_{k=i-h+1}^i (X_{t_k} - \hat{m}(t_i, h))^2$ and $\hat{m}(t_i, h) = \frac{1}{h} \sum_{k=i-h+1}^i X_{t_k}$. Figure 1.1 depicts the rolling estimate of kurtosis along with a time-differenced estimate, calculated as $\{K(t_i, h) - K(t_{i-1}, h) : i = h, h + 1, \dots, N\}$, using a bandwidth of $h = 250$ days for the time period 1990-01-01 to 2015-12-31. Under this bandwidth, the differenced series represents the change in estimated kurtosis caused by moving the rolling estimate one day forward for (approximately) the last year's worth of data. Additionally, we superimpose

an overall estimate of kurtosis (calculated over the entire time period) along with that of the Normal distribution. Based on the overall estimate, the sample

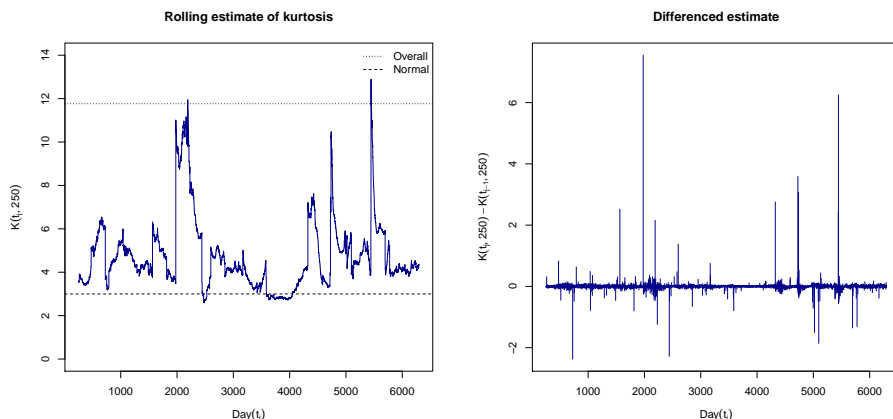


FIGURE 1.1. Rolling estimate of kurtosis calculated using a bandwidth of $h = 250$ days on daily log-returns of the S&P 500 index for the time period 1990-01-01 to 2015-12-31 (left) and the corresponding time-differenced rolling estimate (right).

kurtosis clearly exceeds that of the Normal distribution. However, the one year rolling estimate reveals that although the kurtosis of the log-returns series is typically higher than that of a Normal distribution, the size of the overall estimate can be attributed to the occurrence of a number of extreme return events. These events manifest as sudden spikes in the rolling estimate of kurtosis which can be clearly seen in the time-differenced estimate. In order to account for such extreme events [Merton \(1976\)](#) for example proposed the inclusion of jumps in the diffusion trajectory in order to create a more accurate model of asset price returns than is predicted by the continuous paths of geometric Brownian motion, in which case the modified stochastic differential equation (SDE) assumes the form

$$d \log(X_t) = (\mu - 0.5\sigma^2)dt + \sigma dB_t + \dot{z}_t dN_t, \tag{1.4}$$

where \dot{z}_t denotes a normally distributed jump random variable and N_t is a Poisson process with constant intensity i.e., $N_t - N_s \sim \text{Poi}(\lambda(t - s))$. Under this formulation, extreme events are explicitly included in the stochastic differential equation as randomly occurring discontinuous jumps in the diffusion trajectory. Consequently, the disparity between observed tail behaviour of log-returns and that of Brownian motion is mitigated by the inclusion of a jump mechanism. Building on this, one may extend the model in order to formulate a stochastic volatility model with jumps, for example:

$$\begin{aligned} d \log(X_t) &= \left(\mu - \frac{1}{2}\sigma_t^2\right)dt + \sigma_t dB_t^{(1)} + \dot{z}_t^{(1)} dN_t \\ d\sigma_t^2 &= a(\sigma_t^2, t)dt + b(\sigma_t^2, t)dB_t^{(2)} + \dot{z}_t^{(2)} dN_t, \end{aligned} \tag{1.5}$$

where jumps affect both returns and volatility at the same time. Using this, the useful properties of stochastic volatility specification are retained whilst directly accounting for extreme return events and jumps in volatility.

Although the addition of a jump mechanism serves to improve the flexibility of diffusion models and allows for the formulation of more realistic models of real-world processes, this flexibility comes at the cost of magnifying the already significant difficulties associated with the calculus of diffusion processes. Consequently, the space of analytically tractable jump diffusion models is even more sparse than that of the jump-free diffusion processes. Furthermore, where analytical solutions to quantities such as the transitional density are available, they are often precluded by simplifying assumptions on the specification of both the diffusion part of the process as well as the jump mechanism of the model process. That said, a number of different jump mechanisms have been proposed in the literature: [Ball and Torous \(1985\)](#) propose log-normally distributed jumps under geometric Brownian motion as a model for stock price returns, whilst [Ramezani and Zeng \(1998\)](#) and [Kou \(2002\)](#) assume the same model opting instead for a double-exponential jump distribution. Although the choice of distribution is usually based on some *a priori* information of the process to be modelled, choosing a valid jump distribution can be a subtle process. For example, in the case of [Ball and Torous \(1985\)](#) it is actually meant that the log of the underlying process has normally distributed jumps (i.e., Brownian motion with drift and normally distributed jumps), implying that both the diffusion and jump dynamics are based on the Normal distribution. In this case, [Honore \(1998\)](#) notes that depending on the quality of the data it can be difficult to distinguish which source of randomness is responsible for a random innovation in the underlying process, thus making it difficult to calculate reliable parameter estimates for such a model despite the relatively simple structure of the model.

Despite the limited set of analytically tractable jump diffusion models, numerous estimation techniques have been proposed for jump diffusion models with analytically intractable dynamics. [Eraker \(2001\)](#) apply Monte Carlo techniques, replacing missing sample paths with simulated trajectories (see also [Eraker, Johannes and Polson \(2003\)](#) and [Eraker \(2004\)](#)) in order to estimate the likelihood, thus circumventing the need for closed-form solutions to the likelihood function. Other notable approaches include the efficient method of moments (EMM) scheme of [Gallant, Hsieh and Tauchen \(1997\)](#) which was later used by [Craine, Lochstoer and Syrtveit \(2000\)](#) to perform inference on multivariate jump diffusions, and the empirical characteristic function estimation schemes of [Jiang and Knight \(2002\)](#) and [Rockinger and Semenova \(2005\)](#). [Yu \(2007\)](#) extended the popular Hermite series approximations for jump-free diffusions ([Aït-Sahalia, 2002](#); [Aït-Sahalia et al., 2008](#)) in order to calculate closed-form likelihood approximations for multivariate jump diffusions whilst [Zhang and Schmidt \(2016\)](#) develop short horizon density approximations based on expansions of the characteristic function which can subsequently be used to approximate the likelihood function. Although most of the literature on the estimation of jump diffusion models are concerned with parametric inference, non-parametric techniques have also been developed by [Johannes \(1999\)](#); [Bandi and Nguyen \(2003\)](#) and [Aït-Sahalia,](#)

Fan and Peng (2009). In addition to traditional parametric and non-parametric methods, technical aspects regarding the nature of jump mechanisms in the context of inference have also been explored. For example, Aït-Sahalia (2004) shows how to separate the diffusion and jump dynamics for a given jump diffusion model, whilst Aït-Sahalia et al. (2009) and Aït-Sahalia and Jacod (2011) develop tests for the presence and frequency of jumps in partially observed processes respectively.

In the present paper we develop a procedure for performing likelihood based inference on a class of non-linear, multivariate jump diffusion processes with state-dependent intensity. Using this scheme it is possible to create a rich ecosystem of jump diffusion models that generalise many well-known diffusion models such as the Cox-Ingersoll-Ross (CIR) process (Cox, Ingersoll and Ross, 1985) and Ornstein-Uhlenbeck process (Uhlenbeck and Ornstein, 1930) to the jump diffusion class. Furthermore, the methodology readily allows for the specification of any jump distribution with a known moment structure (e.g., the higher order moments of a Normal or Laplace distribution). The paper is organised as follows: Section 2 outlines theoretical concepts which precede the methodology to follow. Section 3 develops the core methodology of the paper, in which we detail a scheme for approximating the transitional density of a jump diffusion process based on its moment trajectories. Section 4 compares the methodology to existing techniques in the literature for models with near analytically tractable dynamics and subsequently demonstrates how the methodology can be used to conduct inference on jump diffusion models with non-linear dynamics. In Section 6 we apply the methodology to a real-world dataset by fitting various jump diffusion models to Google equity volatility time series. Finally, we give some concluding remarks in Section 7.

2. Multivariate jump diffusions with state-dependent jump intensity

Let \mathbf{P}_t denote a multivariate, k -dimensional pure jump process with dynamics given in differential form by:

$$d\mathbf{P}_t = \mathbf{J}(\mathbf{P}_t, \dot{\mathbf{z}}_t, t)d\mathbf{N}_t, \tag{2.1}$$

where $\mathbf{J}(\mathbf{P}_t, \dot{\mathbf{z}}_t, t) = (\epsilon_{ij}(\mathbf{P}_t, \dot{\mathbf{z}}_t, t))_{k \times q}$ denotes the jump matrix, $\dot{\mathbf{z}}_t = (\dot{z}_t^{(ij)})_{k \times q}$ is a $k \times q$ matrix of random variables with statistically independent columns, $\mathbf{N}_t = (N_t^{(j)})_{q \times 1}$ is a q -dimensional counting process with intensity vector $\boldsymbol{\lambda}(\mathbf{P}_t, \dot{\mathbf{r}}_t, t) = (\lambda_j(\mathbf{P}_t, \dot{\mathbf{r}}_t, t))_{q \times 1}$, and $\dot{\mathbf{r}}_t$ is a q -dimensional stochastic process on which the intensity vector may depend. Under this formulation, the jump matrix relates discrete increments in the process \mathbf{N}_t into non-discrete changes in state of the process \mathbf{P}_t . This is achieved by mapping the discrete increments to real-valued increments through realisations of the jump variables, $\dot{\mathbf{z}}_t$. In turn the mapping is governed by the jump matrix $\mathbf{J}(\mathbf{P}_t, \dot{\mathbf{z}}_t, t)$, which determines how the jump variables enter the process and how the mapping depends on the current state of the process. For example, if the first element of the process \mathbf{N}_t increments at time τ , then every element of \mathbf{P}_τ changes in accordance to the outcome of the first

column of the jump-matrix, which in turn is determined by the functional relation between the first column of jump variables in \mathbf{z}_τ and \mathbf{P}_τ through $\mathbf{J}(\mathbf{P}_\tau, \dot{\mathbf{z}}_\tau, \tau)$. To see this, it is useful to write the process $\mathbf{P}_t = \{P_t^{(1)}, P_t^{(2)}, \dots, P_t^{(k)}\}'$ in terms of its individual components as:

$$P_t^{(i)} = \sum_{j=1}^q \sum_{l=0}^{N_t^{(j)}} \epsilon_{ij}(\mathbf{P}_t, \dot{\mathbf{z}}_t^{(j),l}, t) \quad \text{for } i = 1, 2, \dots, k, \quad (2.2)$$

where $\dot{\mathbf{z}}_t^{(j),l}$ denotes the l -th realisation of the j -th column of the jump variable matrix $\dot{\mathbf{z}}_t^{(j)} = \{\dot{z}_t^{(1j)}, \dot{z}_t^{(2j)}, \dots, \dot{z}_t^{(kj)}\}'$ with distribution function ϕ_j . $P_t^{(i)}$ thus consists of the sum of all jump realisations that have occurred upto and including time t for the i -th dimension, across all q counting process elements of \mathbf{N}_t . Figure 2.1 illustrates how the jump process is constructed from a simulated trajectory for $k = 1$ and $q = 2$.

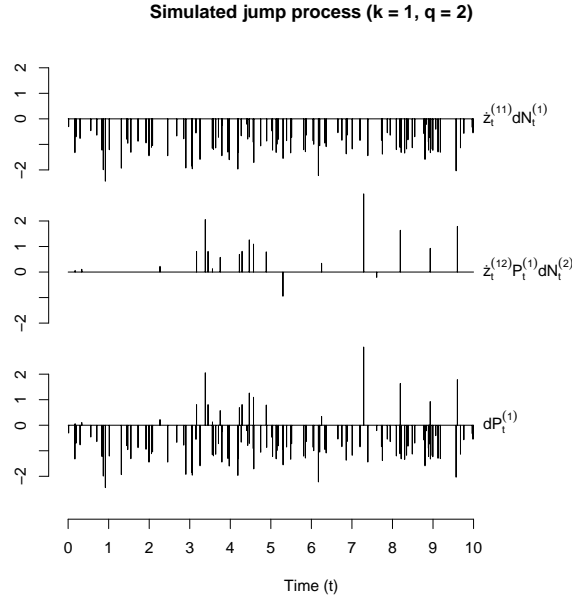


FIGURE 2.1. Construction of the jump process from the increments of individual jump constituents for $k = 1$ and $q = 2$. Here $\epsilon_{11}(P_t^{(1)}, \dot{z}_t^{(11)}, t) = z_t^{(11)}$ with $z_t^{(11)} \sim N(-1, 0.5^2)$, $\epsilon_{12}(P_t^{(1)}, \dot{z}_t^{(12)}, t) = z_t^{(12)} P_t^{(1)}$ with $z_t^{(12)} \sim N(0, 0.05^2)$ and $N_t^{(1)}$ and $N_t^{(2)}$ are subject to constant intensity functions, $\lambda_1 = 10$ and $\lambda_2 = 2$, respectively. $P_t^{(1)}$ is constructed by adding the increments of each jump process sequentially as they occur. Consequently the increments of $P_t^{(1)}$ simply reflect the combined increments of the individual jump components.

In addition to the jump constituents, the process is characterised by the rate at which jump realisations occur, i.e., the rate at which increments in each

$N_t^{(j)}$ occur. This is determined by the intensity vector, which is further allowed to depend on an external vector process $\dot{\mathbf{r}}_t$ as well as the current state of the process. For simplicity we will assume that the arrival rate of each of the Poisson components is also restricted to depend on only a single element of the vector $\dot{\mathbf{r}}_t$:

$$\lambda_j(\mathbf{P}_t, \dot{\mathbf{r}}_t, t) = \lambda_j(\mathbf{P}_t, \dot{r}_t^{(j)}, t) \quad (2.3)$$

where $\dot{r}_t^{(j)} \in \dot{\mathbf{r}}_t = \{\dot{r}_t^{(1)}, \dot{r}_t^{(2)}, \dots, \dot{r}_t^{(k)}\}'$ and each $\dot{r}_t^{(j)}$ evolves according to a distribution function π_j . \mathbf{P}_t thus represents a pure jump process that is characterised by the distributions of the jump-variables and the intensity processes which dictate the rate at which jump realisations occur. The purpose of this formulation is to encompass a class of jump processes with both state-dependent and stochastic intensity, whilst permitting multiple sources of randomness. For example, for $k = 1$ and $q = 2$ the trajectory of the process is subject to two jump sources with possibly distinct dynamics. This may be useful for cases where jumps observed in a real world data have distinct sources with differing distributional characteristics. Likewise, allowing the intensity vector to be stochastic through the process $\dot{\mathbf{r}}_t$, it is possible to formulate a jump mechanism for which the frequency of jump realisations may pass stochastically through high and low intensity phases, which may be useful for modelling jump dynamics over long time periods in financial contexts.

Although pure jump processes are extremely useful modelling tools, a notable deficiency from the perspective of modelling continuously evolving processes is that the process remains dormant in a given state in between successive jump innovations. That is, for phenomena that exhibit jump behaviour but still evolve on small scales in between jumps, the present formulation does not suffice. In order to account for the stochastic evolution of the process between intermittent jumps, one may define a continuous mixture process consisting of a pure jump process and a diffusion process. The dynamics of the resulting k -dimensional jump diffusion $\mathbf{X}_t = \{X_t^{(1)}, X_t^{(2)}, \dots, X_t^{(k)}\}'$ is then governed by the SDE:

$$d\mathbf{X}_t = \boldsymbol{\mu}(\mathbf{X}_t, t)dt + \boldsymbol{\sigma}(\mathbf{X}_t, t)d\mathbf{B}_t + d\mathbf{P}_t, \quad (2.4)$$

where

$$d\mathbf{P}_t = \mathbf{J}(\mathbf{X}_t, \dot{\mathbf{z}}_t, t)d\mathbf{N}_t \quad (2.5)$$

gives the jump mechanism with intensity vector $\boldsymbol{\lambda}(\mathbf{X}_t, \dot{\mathbf{r}}_t, t)$, $\boldsymbol{\mu}(\mathbf{X}_t, t) = (\mu_i(\mathbf{X}_t, t))_{k \times 1}$ gives the instantaneous drift vector, $\boldsymbol{\sigma}(\mathbf{X}_t, t) = (\sigma_{ij}(\mathbf{X}_t, t))_{k \times k}$ is the diffusion matrix of the process and $\mathbf{B}_t = (B_t^{(i)})_{k \times 1}$ is a vector of independent Brownian motions. Equation 2.4 thus constitutes a multivariate jump diffusion with state-dependent jumps and state-dependent and/or stochastic intensity. Consequently, the auxiliary variables contained $\dot{\mathbf{z}}_t$ have the effect of inducing discontinuous jumps in the otherwise continuous paths of the diffusion whenever the counting processes contained in \mathbf{N}_t increment. Furthermore, the rate at which jumps occur may vary according to both the state of the jump diffusion and/or some external process $\dot{\mathbf{r}}_t$. The relationship between the various constituents of the

jump diffusion can more easily be seen by writing equations 2.4 and 2.5 in matrix form:

$$d \begin{bmatrix} X_t^{(1)} \\ \vdots \\ X_t^{(k)} \end{bmatrix} = \begin{bmatrix} \mu_1(\mathbf{X}_t, t) \\ \vdots \\ \mu_2(\mathbf{X}_t, t) \end{bmatrix} dt + \begin{bmatrix} \sigma_{11}(\mathbf{X}_t, t) & \dots & \sigma_{1k}(\mathbf{X}_t, t) \\ \vdots & \ddots & \vdots \\ \sigma_{k1}(\mathbf{X}_t, t) & \dots & \sigma_{kk}(\mathbf{X}_t, t) \end{bmatrix} d \begin{bmatrix} B_t^{(1)} \\ \vdots \\ B_t^{(k)} \end{bmatrix} + d \begin{bmatrix} P_t^{(1)} \\ \vdots \\ P_t^{(k)} \end{bmatrix} \quad (2.6)$$

where

$$d \begin{bmatrix} P_t^{(1)} \\ \vdots \\ P_t^{(k)} \end{bmatrix} = \begin{bmatrix} \epsilon_{11}(\mathbf{X}_t, \dot{z}_t^{(11)}, t) & \dots & \epsilon_{1q}(\mathbf{X}_t, \dot{z}_t^{(1q)}, t) \\ \vdots & \ddots & \vdots \\ \epsilon_{k1}(\mathbf{X}_t, \dot{z}_t^{(k1)}, t) & \dots & \epsilon_{kq}(\mathbf{X}_t, \dot{z}_t^{(kq)}, t) \end{bmatrix} d \begin{bmatrix} N_t^{(1)} \\ \vdots \\ N_t^{(q)} \end{bmatrix}. \quad (2.7)$$

Since Equation 2.4 is formulated in continuous time, the SDE can also be interpreted by relating the coefficients of the equation to its instantaneous moments: Let $\Gamma(\mathbf{X}_t, t) = (\gamma_{ij}(\mathbf{X}_t, t))_{k \times k} = \boldsymbol{\sigma}(\mathbf{X}_t, t)\boldsymbol{\sigma}'(\mathbf{X}_t, t)$ denote the covariance matrix of the diffusion. Given a jump SDE of the form of Equation 2.4, we have for $i, j = 1, 2, \dots, k$:

$$\lim_{h \rightarrow 0} \frac{E[X_{t+h}^{(i)} - X_t^{(i)} | \mathbf{X}_t]}{h} = \mu_i(\mathbf{X}_t, t) + \sum_{m=1}^q E_{\dot{z}}[\epsilon_{im}(\mathbf{X}_t, \dot{z}_t, t)] E_{\dot{r}}[\lambda_m(\mathbf{X}_t, \dot{r}_t, t)] \quad (2.8)$$

and for $v + w \geq 2$

$$\begin{aligned} \lim_{h \rightarrow 0} \frac{E[(X_{t+h}^{(i)} - X_t^{(i)})^v (X_{t+h}^{(j)} - X_t^{(j)})^w | \mathbf{X}_t]}{h} = \\ \gamma_{ij}(\mathbf{X}_t, t) \mathbb{I}(v + w = 2) + \sum_{m=1}^q E_{\dot{z}}[\epsilon_{im}(\mathbf{X}_t, \dot{z}_t, t)^v \epsilon_{jm}(\mathbf{X}_t, \dot{z}_t, t)^w] E_{\dot{r}}[\lambda_m(\mathbf{X}_t, \dot{r}_t, t)]. \end{aligned} \quad (2.9)$$

Interestingly, equations 2.8 and 2.9 indicate that, on an infinitesimal scale, although the first two moments of a jump diffusion is dictated by a mixture of the diffusion and jump dynamics, the higher order instantaneous moments are completely determined by the jump mechanism of the process.

Although the instantaneous dynamics of jump diffusion processes have both theoretical and practical applications, in the context of parametric inference we are often interested in the dynamical behaviour of the process over finite time horizons. As such, a pivotal quantity of interest in the analysis of jump diffusions is the evolution of the transitional density over time. Let $\{S \subseteq \mathbb{R}^k, \mathcal{X}, f\}$, $\{\Psi_j, \mathcal{Z}_j, \phi_j\}_j$ and $\{\Omega_j, \mathcal{L}_j, \pi_j\}_j$ be probability spaces for $j = 1, 2, \dots, q$ then the transitional density $f(\mathbf{X}_t | \mathbf{X}_s)$ of the process \mathbf{X}_t at time t starting in \mathbf{X}_s at time

s is given by the Kolmogorov forward equation (Hanson, 2007):

$$\begin{aligned}
\frac{\partial}{\partial t} f(\mathbf{X}_t | \mathbf{X}_s) = & \\
& - \sum_{i=1}^k \frac{\partial}{\partial X_t^{(i)}} \mu_i(\mathbf{X}_t, t) f(\mathbf{X}_t | \mathbf{X}_s) + \sum_{i=1}^k \sum_{j=1}^k \frac{\partial^2}{\partial X_t^{(i)} \partial X_t^{(j)}} \gamma_{ij}(\mathbf{X}_t, t) f(\mathbf{X}_t | \mathbf{X}_s) \\
& + \sum_{j=1}^q \int_{\Psi_j} \int_{\Omega_j} \lambda_j(\nabla(\mathbf{X}_t, \dot{\mathbf{z}}_t)^{(j)}, \dot{r}_t^{(j)}, t) f(\nabla(\mathbf{X}_t, \dot{\mathbf{z}}_t)^{(j)} | \mathbf{X}_s) |\delta_j(\dot{\mathbf{z}}_t)| d\pi_j(\dot{r}_t^{(j)}) d\phi_j(\dot{\mathbf{z}}_t^{(j)}) \\
& - \sum_{j=1}^q \int_{\Psi_j} \int_{\Omega_j} \lambda_j(\mathbf{X}_t, \dot{r}_t^{(j)}, t) f(\mathbf{X}_t | \mathbf{X}_s) d\pi_j(\dot{r}_t^{(j)}) d\phi_j(\dot{\mathbf{z}}_t^{(j)})
\end{aligned} \tag{2.10}$$

where $(\cdot)^{(j)}$ again denotes the j -th column of a matrix and the elements $\nabla(\mathbf{X}_t, \dot{\mathbf{z}}_t)^{(j)} = \boldsymbol{\nu}_j(\mathbf{X}_t + \mathbf{J}(\mathbf{X}_t, \dot{\mathbf{z}}_t)^{(j)}) = (\nu_{ij}(X_t^{(i)} + \epsilon_{ij}(\mathbf{X}_t, \dot{\mathbf{z}}_t)))_{k \times 1}$ and $|\delta_j(\dot{\mathbf{z}}_t)|$ have special meaning: The role of the function $\boldsymbol{\nu}_j(\mathbf{X}_t + \mathbf{J}(\mathbf{X}_t, \dot{\mathbf{z}}_t)^{(j)})$ is to map jumps in such a way that the state of the process at time t , \mathbf{X}_t , is reached as the result of a jump occurrence at an instant just prior to t . $\boldsymbol{\nu}_j(\mathbf{X}_t + \mathbf{J}(\mathbf{X}_t, \dot{\mathbf{z}}_t)^{(j)})$ thus has the action of reverting the state of the process to that which it was ‘before’ the jump occurrence. For example, if the jump matrix is independent of the process level and $\mathbf{J}(\mathbf{X}_t, \dot{\mathbf{z}}_t)^{(j)} = \dot{\mathbf{z}}_t^{(j)}$, then $\boldsymbol{\nu}_j(\mathbf{X}_t + \dot{\mathbf{z}}_t^{(j)}) = \mathbf{X}_t - \dot{\mathbf{z}}_t^{(j)}$. In turn, $|\delta_j(\dot{\mathbf{z}}_t)|$ acts as the Jacobian resulting from the inversion. For example, following $\mathbf{J}(\mathbf{X}_t)^{(j)} = \dot{\mathbf{z}}_t^{(j)}$, $|\delta_j(\dot{\mathbf{z}}_t)| = 1$. In order for Equation 2.10 to be well defined, we require boundary conditions on the equation. Similarly to jump-free diffusions, the initial conditions for Equation 2.10 are given by the multivariate Dirac delta function $f(\mathbf{x}_s | \mathbf{X}_s) = \delta(\mathbf{x}_s - \mathbf{X}_s)$ where

$$\delta(\mathbf{x}) = \begin{cases} \infty & \text{if } \mathbf{x} = \mathbf{0}, \\ 0 & \text{otherwise.} \end{cases} \tag{2.11}$$

However, due to the presence of the jump mechanism, we also require initial values for the jump components $\{\dot{r}_j(s) = \dot{r}_s, N_j(s) = 0 : j = 1, 2, \dots, q\}$ and any additional time dependences – which we take to have known values at time s .

Although PDDEs such as the Kolmogorov equations are extremely difficult to analyse and solve, the transitional density forms the principal constituent to numerous techniques in the analysis of diffusion processes. In the sections that follow we develop a scheme for calculating approximate solutions to Equation 2.10 for time-inhomogeneous, non-linear jump diffusions, making it possible to analyse a wide spectrum of jump diffusion models.

3.3. A Scalar Example

In order to demonstrate the use of the moment equations in analysing a jump diffusion model, we consider a non-linear, time-inhomogeneous jump diffusion with stochastic intensity. Let:

$$\begin{aligned} dX_t &= \kappa_x(\mu_x - X_t)dt + \sigma_x(1 + 0.4 \sin(\pi t))\sqrt{X_t}dB_t + dP_t \\ dP_t &= \dot{z}_t dN_t \end{aligned} \quad (3.46)$$

with $\dot{z}_t \sim N(\mu_z, \sigma_z^2)$ and $\lambda(X_t, \dot{r}_t, t) = \dot{r}_t$ where the intensity parameter \dot{r}_t has dynamics given by a continuous time Markov chain (CTMC):

$$\dot{r}_t = \begin{cases} \lambda_1 & \text{Low jump frequency,} \\ \lambda_2 & \text{High jump frequency,} \end{cases} \quad (3.47)$$

with transition rate matrix

$$R = \begin{pmatrix} -\beta_1 & \beta_1 \\ \beta_2 & -\beta_2 \end{pmatrix}. \quad (3.48)$$

Under the dynamics of Equation 3.46 the process exhibits linear drift and state-dependent volatility which varies periodically over time. In addition, the process is subject to randomly occurring jump events for which the jump intensity switches stochastically over time between levels λ_1 and λ_2 . Since Equation 3.46 is nested within the scalar generalised quadratic framework we may derive the moment equations of the process directly from Equation 3.27. In order to do so we need to evaluate the expectation of the intensity process over time. From the transition probability matrix of \dot{r}_t , the appropriate expression follows:

$$E(\dot{r}_t) = \begin{cases} \lambda_1 \frac{\beta_2 + \beta_1 e^{-(\beta_1 + \beta_2)(t-s)}}{\beta_1 + \beta_2} + \lambda_2 \frac{\beta_1(1 - e^{-(\beta_1 + \beta_2)(t-s)})}{\beta_1 + \beta_2} & \text{if } \dot{r}_s = \lambda_1, \\ \lambda_2 \frac{\beta_1 + \beta_2 e^{-(\beta_1 + \beta_2)(t-s)}}{\beta_1 + \beta_2} + \lambda_1 \frac{\beta_2(1 - e^{-(\beta_1 + \beta_2)(t-s)})}{\beta_1 + \beta_2} & \text{if } \dot{r}_s = \lambda_2. \end{cases} \quad (3.49)$$

Consequently, the moment equations for model 3.46 under a 6-th order truncation can be verified as:

$$\begin{aligned} m'_1(t) &= \kappa_x \mu_x - \kappa_x m_1(t) + j_1(t) \\ m'_2(t) &= 2(\kappa_x \mu_x m_1(t) - \kappa_x m_2(t)) + \sigma_x^2(1 + 0.4 \sin(\pi t))^2 m_1(t) + j_2(t) \\ m'_3(t) &= 3(\kappa_x \mu_x m_2(t) - \kappa_x m_3(t)) + \sigma_x^2(1 + 0.4 \sin(\pi t))^2 3m_2(t) + j_3(t) \\ m'_4(t) &= 4(\kappa_x \mu_x m_3(t) - \kappa_x m_4(t)) + \sigma_x^2(1 + 0.4 \sin(\pi t))^2 6m_3(t) + j_4(t) \\ m'_5(t) &= 5(\kappa_x \mu_x m_4(t) - \kappa_x m_5(t)) + \sigma_x^2(1 + 0.4 \sin(\pi t))^2 10m_4(t) + j_5(t) \\ m'_6(t) &= 6(\kappa_x \mu_x m_5(t) - \kappa_x m_6(t)) + \sigma_x^2(1 + 0.4 \sin(\pi t))^2 15m_5(t) + j_6(t) \end{aligned} \quad (3.50)$$

with $m_i(s) = X_s^i$ for $i = 1, 2, \dots, 6$ where

$$\begin{aligned}
 j_1(t) &= h(t, \boldsymbol{\lambda}, \boldsymbol{\beta})\rho_1 \\
 j_2(t) &= h(t, \boldsymbol{\lambda}, \boldsymbol{\beta})(2\rho_1m_1(t) + \rho_2) \\
 j_3(t) &= h(t, \boldsymbol{\lambda}, \boldsymbol{\beta})(3\rho_1m_2(t) + 3\rho_2m_1(t) + \rho_3) \\
 j_4(t) &= h(t, \boldsymbol{\lambda}, \boldsymbol{\beta})(4\rho_1m_3(t) + 6\rho_2m_2(t) + 4\rho_3m_1(t) + \rho_4) \\
 j_5(t) &= h(t, \boldsymbol{\lambda}, \boldsymbol{\beta})(5\rho_1m_4(t) + 10\rho_2m_3(t) + 10\rho_3m_2(t) + 5\rho_4m_1(t) + \rho_5) \\
 j_6(t) &= h(t, \boldsymbol{\lambda}, \boldsymbol{\beta})(6\rho_1m_5(t) + 15\rho_2m_4(t) + 20\rho_3m_3(t) + 15\rho_4m_2(t) + 6\rho_5m_1(t) + \rho_6),
 \end{aligned} \tag{3.51}$$

and

$$h(t, \boldsymbol{\lambda}, \boldsymbol{\beta}) = \lambda_1 \frac{\beta_2 + \beta_1 e^{-(\beta_1 + \beta_2)(t-s)}}{\beta_1 + \beta_2} + \lambda_2 \frac{\beta_1(1 - e^{-(\beta_1 + \beta_2)(t-s)})}{\beta_1 + \beta_2}. \tag{3.52}$$

Here, the relation between the elements $\rho_1, \rho_2, \dots, \rho_6$ and the parameters μ_z and σ_z follow straightforwardly from the non-central moments of the Normal distribution. The effect of the jump mechanism on the moments of the diffusion can immediately be seen through Equation 3.50 where the $j_i(t)$ dictate how the intensity and jump parameters feed into the moment structure of the process. For example, when $\mu_z = 0$ it follows that $\rho_1 = 0$ and the mean trajectory of the process remains unchanged from that of the jump-free process. Idiosyncrasies aside, by solving Equation 3.50 we may evaluate the moment trajectories of Equation 3.46 over time. When the model structure is not too complicated, this can be achieved using standard techniques for evaluating systems of differential equations. For large truncation orders this may involve the use of a computer algebra system (CAS) in order to calculate Laplace transforms for elements of the moment equations. Alternatively, when the moment equations involve non-linear terms and/or complicated time-inhomogeneous terms, standard numerical techniques can be used in order to solve the resulting system of moment equations. For our purposes we employ high-order Runge-Kutta schemes such as the Runge-Kutta-Fehlberg (4)5 method (Fehlberg, 1970) or the (8)10-th order method of Feagin (2007)².

In order to verify that the derived moment equations are indeed valid, we need to perform an independent check on the resulting moment trajectories. For these purposes we can simulate trajectories of Equation 3.46 over the desired transition horizon and calculate moment statistics with which we can compare the relevant quantities. In order to simulate trajectories of Equation 3.46 we apply a Euler-Maruyama scheme to the SDE and subsequently derive an iterative updating scheme that can be used to approximate the trajectory of a jump diffusion at fixed points along a desired transition horizon. For example, let τ be a scalar time index on the transition horizon $[s, t]$ and Δ a finite time step, then an iterative updating scheme for simulating a single trajectory of Equation 3.46 follows:

²Here we use the convention that the term in brackets denotes the embedded order of the method used for calculating local error estimates.

(1) Set $\tau = s$ and initialize the jump diffusion and intensity process X_τ and \dot{r}_τ respectively.

(2) (a) Set:

$$X_{\tau+\Delta} = X_\tau + \mu_i(\mathbf{X}_\tau, \tau)\Delta + \sigma(\mathbf{X}_\tau, \tau)Z, \quad (3.53)$$

by drawing $Z \sim N(0, \Delta)$.

(b) If

$$1 - \exp(\lambda(X_\tau, \dot{r}_\tau, \tau)\Delta) > u \quad (3.54)$$

where $u \sim U(0, 1)$, draw $\dot{z}_\tau \sim N(\mu_z, \sigma_z^2)$ and set

$$X_{\tau+\Delta} = X_{\tau+\Delta} + \dot{z}_\tau. \quad (3.55)$$

(4) Set

$$\dot{r}_{\tau+\Delta} = \begin{cases} \lambda_1 & \text{w.p. } \frac{\beta_2}{\beta_1+\beta_2} - \frac{\beta_2}{\beta_1+\beta_2}e^{-(\beta_1+\beta_2)\Delta} \text{ if } \dot{r}_\tau = \lambda_2, \\ \lambda_2 & \text{w.p. } \frac{\beta_1}{\beta_1+\beta_2} - \frac{\beta_1}{\beta_1+\beta_2}e^{-(\beta_1+\beta_2)\Delta} \text{ if } \dot{r}_\tau = \lambda_1, \\ \dot{r}_\tau & \text{otherwise.} \end{cases} \quad (3.56)$$

(4) Set $\tau = \tau + \Delta$ and if $\tau \leq t$ go to step (2).

For purposes of the experiment, let $\boldsymbol{\theta} = \{\kappa_x, \mu_x, \sigma_x, \mu_z, \sigma_z\} = \{2, 5, 1, 1, 0.25\}$, $\boldsymbol{\lambda} = \{\lambda_1, \lambda_2\} = \{1, 3\}$ and $\boldsymbol{\beta} = \{\beta_1, \beta_2\} = \{0.25, 1\}$ and fix the initial values of the process to $X_0 = 4$ and $\dot{r}_0 = \lambda_1$. Figure 3.1 compares log-scaled simulated moments of Equation 3.46 to those calculated from solving the moment equations numerically. The simulated moments are calculated using 10000 trajectories and a step-size of 0.001 time units. As expected, the simulated moments and moment equations match closely with the mean trajectory of the process (corresponding to $m_1(t)$) being unaffected by the periodicity of the volatility coefficient.

Naturally, the next step in analysing Equation 3.46 is to investigate the transitional density. Indeed, using the moment equations as a basis we can easily approximate the transitional density using a suitable surrogate density. For purposes of this example we make use of the scalar saddlepoint approximation:

$$f(X_t|X_s) \approx f_{SPT}^{(d)}(X_t|X_s) = \frac{1}{\sqrt{2\pi \frac{\partial^2}{\partial \alpha^2} K^{(d)}(\alpha_0, t)}} \exp\left(\frac{\partial}{\partial \alpha} K^{(d)}(\alpha_0, t) - \alpha_0 X_t\right), \quad (3.57)$$

where

$$K^{(d)}(\alpha, t) = \sum_{i=1}^d \frac{\alpha^i \kappa_i(t)}{i!}, \quad (3.58)$$

α_0 solves

$$\frac{\partial^2}{\partial \alpha^2} K^{(d)}(\alpha, t) = X_t, \quad (3.59)$$

$\kappa_i(t)$ denotes the i -th cumulant of the process at time t , and d denotes the truncation order of the approximation. Thus, by using the appropriate moment-cumulant relations we can easily employ the saddlepoint approximation in

order to approximate the transitional density. Figure 3.2 compares the resulting approximation to the frequency distribution calculated from the simulated trajectories at various points in time. As with the moment equations, the transition density approximation appears to accurately replicate the transition density at the indicated time epochs. The effect of the periodic volatility can clearly be seen in the oscillating shape of the transition density surface.

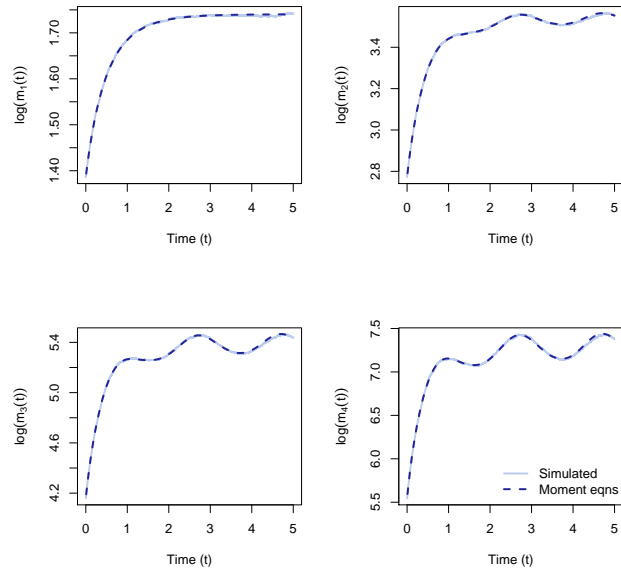


FIGURE 3.1. Log-scaled simulated moment trajectories (solid, light blue) and approximate moment equations (dashed, dark blue) for the first four non-central moments of Equation 3.46 over time.

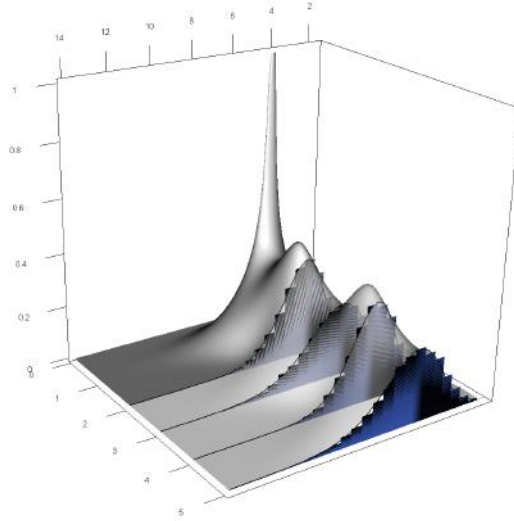


FIGURE 3.2. Approximate transition density (gray/lightgray) of Equation 3.46 and simulated transition density (light blue - dark blue) at times $t = 2$, $t = 3$, $t = 4$ and $t = 5$. The transition density surface is highlighted in black for each epoch of the comparison.

By repeating the calculation of the transition density approximation for a different set of initial conditions – where instead of starting in the low jump frequency state, we let the process start in the high jump frequency state – we can visualize the effect of the stochastic intensity. Figure 3.3 compares the approximate transition densities for the two initial states of the intensity process. Under the high intensity regime the transition density is significantly more skewed than under the low intensity regime. This follows intuitively since, although the jump distribution remains fixed regardless of the state of the intensity process, under the assumed parameter set jumps will typically assume positive values. Consequently, if jumps occur more frequently the process is likely to have propagated further from its initial state at a given time than under the low intensity regime. Noting that, despite there being a non-zero probability of the intensity process switching back to the low intensity state, on average the intensity is expected to be higher for the duration of the transition horizon than compared to starting from the low intensity state. Indeed, this can be verified by comparing $h(t, \boldsymbol{\lambda}, \boldsymbol{\beta})$ for both initial states of the intensity process under the assumed parameter set.

Parameter	True Value	Estimate	90% CI
μ_x	0.50	0.54	(0.39, 0.68)
β_x	2.00	1.92	(1.47, 2.33)
σ_x	0.10	0.11	(0.10, 0.11)
μ_y	1.00	1.05	(0.92, 1.18)
β_y	5.00	4.96	(4.88, 5.01)
σ_y	0.10	0.11	(0.10, 0.11)
λ	1.00	1.10	(0.82, 1.43)
$\mu_{z_{11}}$	0.50	0.46	(0.30, 0.61)
$\mu_{z_{21}}$	0.50	0.31	(0.21, 0.45)
$\sigma_{z_{11}}$	0.50	0.53	(0.41, 0.70)
$\sigma_{z_{21}}$	0.50	0.55	(0.47, 0.66)

TABLE 2
 Parameter estimates and 90% credibility intervals for Equation 5.10 under the simulated dataset in Figure 5.5.

The resulting parameter estimates match that of the true parameter set quite closely, with the notable exception of $\mu_{z_{21}}$. However, closer inspection reveals that the estimate calculated under the jump diffusion model is indeed a valid estimate as the value calculated from the jump realisations directly is quite similar. Indeed, for this experiment the jump signal is quite strong since the dispersion of the jump distribution is large relative to the diffusion parameters. Consequently, the contrast between the jump and diffusion dynamics is sufficiently high to make quite accurate inference with regard to the dynamics of the jump mechanism. Although the estimated parameters are close to the true parameter set, the particular sequence of jump realisations generated in the simulation contains values which are relatively unlikely under the true parameter set. Despite this, the parameters of the jump mechanism could still be extracted accurately, albeit preserving the attributes of the unlikely jump sequence.

6. Application to Google stock price volatility

In a post sub-prime crisis world, investors have become increasingly aware of the importance of understanding the impact that large movements in equity values can have on portfolios and financial products. As such, techniques in analysing financial data have grown increasingly complex and often focus on better managing the risks and opportunities associated with extreme events, both at the high frequency and low frequency trading spectrum. In conjunction with this, data markets have evolved similarly, with highly detailed data on thousands of economic variables and equities accessible at little to no cost. In keeping with this, the Chicago Board Options Exchange (CBOE) publishes volatility indexes for a number of large-cap stocks listed on major stock exchanges. By using the same principles that underlie established indices such as the S & P 500 volatility index, these equity volatility indices attempt to quantify the evolution of the volatility of individual stock price processes as opposed to that of an index of equities. Indeed, the dynamics of individual stock processes can be vastly

different from that of an aggregated set of stocks. As such, equity volatility indices can be extremely useful in quantifying exposure in portfolios which have large investments in such equities and related processes. By using various jump diffusion models, we attempt to model the equity volatility of internet search giant Google. Figure 6.1 illustrates the trajectory of the Google equity volatility (VXGOG) from its inception in 2010 up to the end of 2015, sampled at daily intervals. For purposes of the analysis that follows we measure time in years and use exact dates for observations in order to construct transition horizons for consecutive observations.

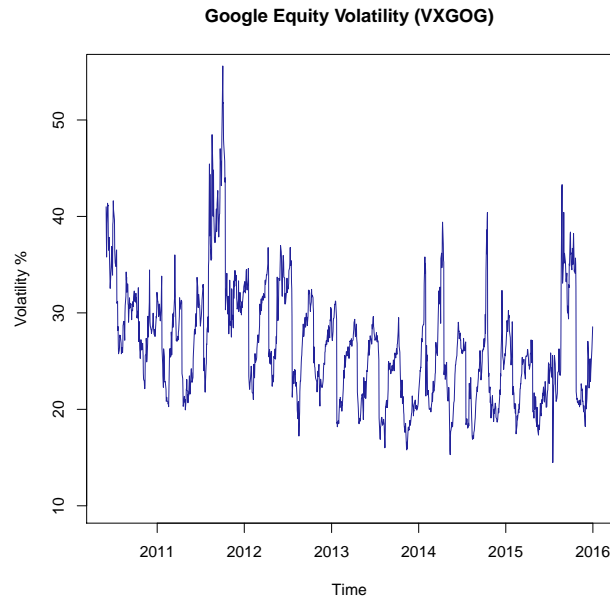


FIGURE 6.1. Daily equity volatility for Google shares for the period 2010-03-11 to 2016-01-01.

In order to model the volatility time-series, we define a number of jump diffusion models nested within the SDE:

$$\begin{aligned} dX_t &= \mu_{\theta}(X_t, t)dt + \sigma_{\theta}(X_t, t)dW_t + dP_t \\ dP_t &= J(X_t, \dot{z}_t)dN_t \end{aligned} \tag{6.1}$$

with jump intensity $\lambda_{\theta}(X_t, t)$, that aim to replicate the salient features and dynamics of the volatility series. Using the generalised quadratic framework of Section ??, we can formulate a template for Equation 6.1 that can be used to fit various forms of drift, diffusion, and jump specifications. For purposes of modelling the drift of the volatility series, we make use of linear mean reverting drift structures of the form:

$$\mu_{\theta}(X_t, t) = \alpha(\beta + h(t, \theta) - X_t). \tag{6.2}$$

Here, $\beta + h(t, \boldsymbol{\theta})$ represents a possibly fluctuating level to which the process reverts over time. Using this formulation we can recover standard mean reversion structures such as the CIR and Ornstein-Uhlenbeck models by setting $h(t, \boldsymbol{\theta}) = 0$ and test for the presence of volatility cycles by replacing $h(t, \boldsymbol{\theta})$ with a periodic function. For example in this case, we let

$$h(t, \nu_1, \nu_2) = \nu_1 \sin(8\pi(t + 0.25(\nu_2 - 0.5))) \quad (6.3)$$

for $\nu_1 > 0$ and $\nu_2 \in [0, 1]$, which specifies a quarterly volatility cycle. Due to the mean reverting structure, the model process will subsequently have long-run mean dynamics that mimic the behaviour of the term $\beta + h(t, \nu_1, \nu_2)$. For purposes of modelling the diffusion dynamics of the volatility series we assume various forms for the diffusion coefficient where

$$\sigma_{\boldsymbol{\theta}}(X_t, t) = \begin{cases} \sigma & \text{for constant volatility,} \\ \sigma\sqrt{X_t} & \text{for linear instantaneous variance,} \\ \sigma X_t & \text{for quadratic instantaneous variance.} \end{cases} \quad (6.4)$$

Similarly, in order to model the jump dynamics of the process, we alternate between combinations of constant and state dependence coefficients of the jump mechanism where the intensity coefficient is defined as

$$\lambda_{\boldsymbol{\theta}}(X_t, t) = \begin{cases} \kappa & \text{for constant intensity,} \\ \kappa X_t & \text{for relative intensity,} \end{cases} \quad (6.5)$$

and the jump coefficient assumes the form

$$J(X_t, \dot{z}_t) = \begin{cases} \dot{z}_t & \text{for constant jump size,} \\ \dot{z}_t X_t & \text{for relative jump size,} \end{cases} \quad (6.6)$$

and it is assumed that jumps are normally distributed i.e.,

$$\phi(\dot{z}_t, \mu_z, \sigma_z^2) = N(\mu_z, \sigma_z^2) = \frac{1}{\sqrt{2\pi\sigma_z^2}} \exp\left(-\frac{(\dot{z}_t - \mu_z)^2}{2\sigma_z^2}\right). \quad (6.7)$$

Table 3 gives various forms of drift, diffusion and jump mechanisms fitted to the VXGOG series. Using the methodology of sections 3 and 5 in conjunction with the RWMH algorithm, we are able to efficiently calculate parameter estimates and deviance information criterion (DIC) statistics for the various model specifications. For each case we place prior distributions on the parameters of the model as indicated in Table 4. For reference, we also include a sample jump-free models that fit within the forgoing assumptions. Corresponding parameter estimates and 90% credibility intervals are given in tables 5 - 7.

Mod.	$\mu(X_t, t)$	$\sigma(X_t, t)$	$\lambda(X_t, t)$	$J(X_t, \dot{z}_t)$	$\dot{z}_t \sim$	DIC	p_D
1	$\alpha(\beta - X_t)$	σ	\cdot	\cdot	\cdot	5776.10	2.77
2	$\alpha(\beta - X_t)$	$\sigma\sqrt{X_t}$	\cdot	\cdot	\cdot	5627.37	2.99
3	$\alpha(\beta - X_t)$	σX_t	\cdot	\cdot	\cdot	5482.72	3.22
4	$\alpha(\beta - X_t)$	$\sigma\sqrt{X_t}$	κ	\dot{z}_t	$N(\mu_z, \sigma_z^2)$	4832.27	6.28
5	$\alpha(\beta - X_t)$	σX_t	κ	\dot{z}_t	$N(\mu_z, \sigma_z^2)$	4798.80	5.69
6	$\alpha(\beta - X_t)$	σX_t	κX_t	\dot{z}_t	$N(\mu_z, \sigma_z^2)$	4784.03	5.61
7	$\alpha(\beta - X_t)$	σX_t	κ	$\dot{z}_t X_t$	$N(\mu_z, \sigma_z^2)$	4778.91	6.16
8	$\alpha(\beta + h(t, \nu_1, \nu_2) - X_t)$	σX_t	κ	\dot{z}_t	$N(\mu_z, \sigma_z^2)$	4767.67	8.35
9	$\alpha(\beta + h(t, \nu_1, \nu_2) - X_t)$	σX_t	κX_t	\dot{z}_t	$N(\mu_z, \sigma_z^2)$	4752.46	8.30
10	$\alpha(\beta + h(t, \nu_1, \nu_2) - X_t)$	σX_t	κ	$\dot{z}_t X_t$	$N(\mu_z, \sigma_z^2)$	4744.02	7.54

TABLE 3

Various drift, diffusion, and jump mechanism specifications for the Google equity VIX series. Approximate deviance information criterion (DIC) and fitted effective number of parameters (p_D) are also tabulated for each model (minimum DIC value indicated in bold). The results suggest that the observed series exhibits time-inhomogeneous linear drift with state-dependent diffusion. In addition, there is evidence to suggest state-dependence within the jump mechanism of the process.

Parameter	Prior distribution
α	Gamma(0.001, 0.001)
β	Normal(25, 5 ²)
σ^2	Inv-Gamma(0.001, 0.001)
κ	Gamma(0.001, 0.001)
ν_1	Gamma(0.001, 0.001)
ν_2	Beta(0.5, 0.5)

TABLE 4

Prior distributions on the parameter space. Where the relevant terms are included in given model, the corresponding prior distributions are applied. Although the prior distributions used here are mostly weakly informative, the prior distributions on β and ν_2 follow from basic inspection of the time series.

	Model 1		Model 2		Model 3		Model 4	
	Est.	90%CI	Est.	90%CI	Est.	90%CI	Est.	90%CI
α	15.07	(10.63, 19.26)	15.30	(11.30, 19.07)	13.36	(9.82, 17.28)	7.40	(5.10, 9.66)
β	26.40	(24.88, 27.83)	26.50	(25.01, 27.96)	27.04	(25.58, 28.79)	27.49	(25.49, 29.42)
σ	32.77	(31.80, 33.63)	6.10	(5.91, 6.30)	1.12	(1.09, 1.16)	3.38	(3.20, 3.54)
λ	\cdot	\cdot	\cdot	\cdot	\cdot	\cdot	23.97	(18.94, 30.72)
μ_z	\cdot	\cdot	\cdot	\cdot	\cdot	\cdot	-0.42	(-1.20, 0.33)
σ_z	\cdot	\cdot	\cdot	\cdot	\cdot	\cdot	4.90	(4.28, 5.67)

TABLE 5

Parameter estimates and 90% credibility intervals for models 1 to 4. Estimates for each model are calculated from 110000 random walk Metropolis-Hastings updates with a burn-in period of 10000 iterations.

	Model 5		Model 6		Model 7		Model 8	
	Est.	90%CI	Est.	90%CI	Est.	90%CI	Est.	90%CI
α	6.55	(4.24, 8.92)	6.30	(3.57, 9.31)	6.44	(4.03, 8.89)	10.69	(7.25, 13.75)
β	27.95	(25.76, 30.56)	27.97	(25.73, 30.88)	27.71	(25.39, 30.41)	26.97	(25.70, 28.43)
σ	0.67	(0.64, 0.70)	0.66	(0.64, 0.69)	0.65	(0.61, 0.68)	0.66	(0.63, 0.70)
λ	20.47	(14.66, 26.89)	0.85	(0.65, 1.09)	28.60	(21.37, 37.88)	21.52	(15.33, 27.96)
μ_z	-0.50	(-1.39, 0.37)	-0.53	(-1.43, 0.29)	-0.01	(-0.03, 0.01)	-0.35	(-1.26, 0.41)
σ_z	5.17	(4.39, 6.10)	4.93	(4.23, 5.81)	0.15	(0.13, 0.17)	5.03	(4.34, 5.77)
ν_1	6.70	(4.89, 8.82)
ν_2	0.56	(0.52, 0.62)

TABLE 6

Parameter estimates and 90% credibility intervals for models 5 to 8. Estimates for each model are calculated from 110000 random walk Metropolis-Hastings updates with a burn-in period of 10000 iterations.

	Model 9		Model 10	
	Est.	90%CI	Est.	90%CI
α	10.28	(6.84, 13.46)	10.71	(7.76, 14.09)
β	27.03	(25.71, 28.66)	26.72	(25.43, 28.03)
σ	0.66	(0.63, 0.69)	0.64	(0.61, 0.68)
λ	0.88	(0.63, 1.17)	28.09	(20.78, 35.40)
μ_z	-0.31	(-1.15, 0.43)	0.00	(-0.03, 0.02)
σ_z	4.89	(4.13, 5.81)	0.15	(0.13, 0.17)
ν_1	6.74	(4.77, 9.09)	6.53	(4.79, 8.70)
ν_2	0.56	(0.52, 0.61)	0.56	(0.51, 0.61)

TABLE 7

Parameter estimates and 90% credibility intervals for models 9 to 10. Estimates for each model are calculated from 110000 random walk Metropolis-Hastings updates with a burn-in period of 10000 iterations.

Although the model space presented here is by no means exhaustive (the set of models considered here represent the best performing models among a number of additional specifications), the models serve as a basis for testing a number of hypotheses with regard to the volatility series. Using the approximate DIC values as a guide for comparing the various model specifications, we can identify which elements improve model fit and thus which elements most accurately replicate the observed dynamics. Within the jump-free model set, the fit is improved for models with diffusion coefficients which are more sensitive to changes in the state of the process. This suggests that the volatility of the volatility process increases in accordance with the level of the process. Perhaps the greatest improvement in model fit stems from including a jump mechanism in the diffusion model. Although this comes at the cost of three additional parameters, the jump diffusion models fair significantly better than their corresponding jump-free models. Despite the addition of the jump mechanism, model fit is still improved for models with greater state-dependence in volatility. With respect to the jump mechanism itself, there is evidence that jump magnitudes may indeed vary in accordance to the level of the process. Finally, by including a quarterly drift cycle we can further improve model fit.

by assuming that $\kappa_{ij}(t) = 0 \quad \forall \quad i + j > m$ the truncated CGF is given by:

$$K^{(d)}(\alpha, \beta, t) = \sum_{i+j \leq d} \frac{\alpha^i \beta^j}{i!j!} \kappa_{ij}(t). \quad (\text{E.1})$$

For bivariate GQDs under an (even) d -th order truncation, the saddlepoint approximation (Renshaw, 2000) is given by:

$$f_{SPT}^{(d)}(X_t, Y_t | X_s, Y_s) = \frac{\exp(K^{(m)}(\alpha_0, \beta_0) - \alpha_0 X_t - \beta_0 Y_t)}{2\pi \sqrt{\frac{\partial^2 K^{(d)}}{\partial \alpha^2} \frac{\partial^2 K^{(d)}}{\partial \beta^2} - \left(\frac{\partial K^{(d)}}{\partial \alpha \partial \beta}\right)^2}}, \quad (\text{E.2})$$

for

$$\begin{aligned} K^{(d)}(\alpha, \beta) &= \alpha \kappa_{10}(t) + \frac{\alpha^2}{2} \kappa_{20}(t) + \frac{\alpha^3}{6} \kappa_{30}(t) + \frac{\alpha^4}{24} \kappa_{40}(t) + \dots + \frac{\alpha^d}{d!} \kappa_{d0}(t) \\ &+ \beta \kappa_{01}(t) + \frac{\beta^2}{2} \kappa_{02}(t) + \frac{\beta^3}{6} \kappa_{03}(t) + \frac{\beta^4}{24} \kappa_{04}(t) + \dots + \frac{\beta^d}{d!} \kappa_{0d}(t) \\ &+ \alpha \beta \kappa_{11}(t) + \frac{\alpha^2 \beta}{2} \kappa_{21}(t) + \frac{\alpha \beta^2}{2} \kappa_{12}(t) + \dots + \frac{\alpha^{d/2} \beta^{d/2}}{(d/2)!^2} \kappa_{((d/2)(d/2)}(t) + \dots \\ &+ \frac{\alpha^{d-1} \beta}{(d-1)!} \kappa_{(d-1)1}(t) + \frac{\alpha \beta^{d-1}}{(d-1)!} \kappa_{1(d-1)}(t), \end{aligned} \quad (\text{E.3})$$

where α_0 and β_0 solves the system:

$$\begin{aligned} \frac{\partial K^{(d)}}{\partial \alpha}(\alpha, \beta) &= X_t, \\ \frac{\partial K^{(d)}}{\partial \beta}(\alpha, \beta) &= Y_t. \end{aligned} \quad (\text{E.4})$$

Since the saddlepoint approximation requires evaluation of the cumulants, we need relate the respective moments to their cumulant counterparts. Again, this can be achieved using the moment and cumulant relations outlined in Appendix C.

References

- AÏT-SAHALIA, Y. (2002). Maximum Likelihood Estimation of Discretely Sampled Diffusions: A Closed-Form Approximation Approach. *Econometrica* **70** 223-262.
- AÏT-SAHALIA, Y. (2004). Disentangling diffusion from jumps. *Journal of Financial Economics* **74** 487-528.
- AÏT-SAHALIA, Y. et al. (2008). Closed-form Likelihood Expansions for Multivariate Diffusions. *The Annals of Statistics* **36** 906-937.
- AÏT-SAHALIA, Y., FAN, J. and PENG, H. (2009). Nonparametric transition-based tests for jump diffusions. *Journal of the American Statistical Association* **104**.

- AÏT-SAHALIA, Y., JACOD, J. et al. (2009). Testing for jumps in a discretely observed process. *The Annals of Statistics* **37** 184–222.
- AÏT-SAHALIA, Y. and JACOD, J. (2011). Testing whether jumps have finite or infinite activity. *The Annals of Statistics* 1689–1719.
- BALL, C. A. and TOROUS, W. N. (1985). On Jumps in Common Stock Prices and Their Impact on Call Option Pricing. *The Journal of Finance* **40** 155–173.
- BANDI, F. M. and NGUYEN, T. H. (2003). On the Functional Estimation of Jump-Diffusion Models. *Journal of Econometrics* **116** 293–328.
- CARR, P. and MADAN, D. (1999). Option Valuation Using the Fast Fourier Transform. *Journal of Computational Finance* **2** 61–73.
- COX, J. C., INGERSOLL, J. E. and ROSS, S. A. (1985). A Theory of the Term Structure of Interest Rates. *Econometrica* **53** 385–407.
- CRAINE, R., LOCHSTOER, L. A. and SYRTVEIT, K. (2000). Estimation of a Stochastic-Volatility Jump-Diffusion Model. *Revista de Analisis Economico* **15** 61–87.
- ECKNER, A. (2009). Computational Techniques for Basic Affine Models of Portfolio Credit Risk. *Journal of Computational Finance* **13** 63.
- ERAKER, B. (2001). MCMC Analysis of Diffusion Models With Application to Finance. *Journal of Business & Economic Statistics* **19** 177–191.
- ERAKER, B. (2004). Do Stock Prices and Volatility Jump? Reconciling Evidence From Spot and Option Prices. *The Journal of Finance* **59** 1367–1404.
- ERAKER, B., JOHANNES, M. and POLSON, N. (2003). The Impact of Jumps in Volatility and Returns. *The Journal of Finance* **58** 1269–1300.
- FEAGIN, T. (2007). A Tenth-Order Runge-Kutta Method With Error Estimate. In *Proceedings of the IAENG Conference on Scientific Computing*.
- FEHLBERG, E. (1970). Classical Fourth- and Lower Order Runge-Kutta Formulas With Stepsize Control and Their Application to Heat Transfer Problems. *Computing* **6** 61–71.
- FILIPOVIĆ, D., MAYERHOFER, E. and SCHNEIDER, P. (2013). Density Approximations for Multivariate Affine Jump-Diffusion Processes. *Journal of Econometrics* **176** 93–111.
- GALLANT, A. R., HSIEH, D. and TAUCHEN, G. (1997). Estimation of Stochastic Volatility Models With Diagnostics. *Journal of Econometrics* **81** 159–192.
- HANSON, F. B. (2007). *Applied Stochastic Processes and Control for Jump-Diffusions: Modeling, Analysis, and Computation* **13**. SIAM.
- HARVEY, J. R. (1972). On Expressing Moments in Terms of Cumulants and Vice Versa. *The American Statistician* **26** 38–39.
- HONORE, P. (1998). Pitfalls in Estimating Jump-Diffusion Models. *Available at SSRN 61998*.
- JIANG, G. J. and KNIGHT, J. L. (2002). Estimation of Continuous-Time Processes via the Empirical Characteristic Function. *Journal of Business & Economic Statistics* **20**.
- JIN, P., RÜDIGER, B. and TRABELSI, C. (2015). Positive Harris Recurrence and Exponential Ergodicity of the Basic Affine Jump-Diffusion. *arXiv preprint arXiv:1501.03638*.
- JOHANNES, M. (1999). Jumps in Interest Rates: A Nonparametric Approach.

Journal of Finance.

- KOU, S. G. (2002). A Jump-Diffusion Model for Option Pricing. *Management Science* **48** 1086–1101.
- KREY, S., LIGGES, U. and MERSMANN, O. (2011). **fftw**: Fast FFT and DCT Based on FFTW R package version 1.0-3.
- MERTON, R. C. (1976). Option pricing when underlying stock returns are discontinuous. *Journal of Financial Economics* **3** 125–144.
- PIENAAR, E. A. D. and VARUGHESE, M. M. (2015a). **DiffusionRgqd**: An R Package for Performing Inference and Analysis on Time-Inhomogeneous Quadratic Diffusion Processes R package version 0.1.2.
- PIENAAR, E. A. D. and VARUGHESE, M. M. (2015b). **DiffusionRjgqd**: An R Package for Performing Inference and Analysis on Time-Inhomogeneous Quadratic Jump Diffusions with State-Dependent Intensity R package version 0.1.1.
- R CORE TEAM (2015). R: A Language and Environment for Statistical Computing R Foundation for Statistical Computing, Vienna, Austria.
- RAMEZANI, C. A. and ZENG, Y. (1998). Maximum likelihood estimation of asymmetric jump-diffusion processes: Application to security prices. *Available at SSRN 606361*.
- RENSHAW, E. (2000). Applying the Saddlepoint Approximation to Bivariate Stochastic Processes. *Mathematical Biosciences* **168** 57–75.
- ROCKINGER, M. and SEMENOVA, M. (2005). Estimation of jump-diffusion processes via empirical characteristic functions. *Available at SSRN 770785*.
- UHLENBECK, G. E. and ORNSTEIN, L. S. (1930). On the Theory of the Brownian Motion. *Physical Review* **36** 823.
- YU, J. (2007). Closed-form likelihood approximation and estimation of jump-diffusions with an application to the realignment risk of the Chinese Yuan. *Journal of Econometrics* **141** 1245–1280.
- ZHANG, L. and SCHMIDT, W. M. (2016). An approximation of small-time probability density functions in a general jump diffusion model. *Applied Mathematics and Computation* **273** 741–758.